



ELSEVIER

25 May 2000

OPTICS  
COMMUNICATIONS

Optics Communications 179 (2000) 13–18

www.elsevier.com/locate/optcom

# Identification of nonclassical states in neutron spin precession experiments

G. Badurek<sup>a</sup>, H. Rauch<sup>b,\*</sup>, M. Suda<sup>c</sup>, H. Weinfurter<sup>d</sup><sup>a</sup> *Institut für Kernphysik, Technische Universität, Stadionallee 2, A-1020 Wien, Austria*<sup>b</sup> *Atominstytut der Österreichischen Universitäten, Stadionallee 2, A-1020 Wien, Austria*<sup>c</sup> *Österreichisches Forschungszentrum, A-2444 Seibersdorf, Austria*<sup>d</sup> *Sektion Physik, Ludwig-Maximilians-Universität, Schellingstr 3 / 4, 80799 München, Germany*

Received 4 February 2000; accepted 16 February 2000

## Abstract

Highly non-classical states are produced in polarized neutron spin precession experiments due to the coherent superposition of spin-up and spin-down states. These states are described within the Wigner function formalism and the measured momentum modulation in a neutron spin precession experiment is taken as a sign of such non-classical states. © 2000 Elsevier Science B.V. All rights reserved.

PACS: 03.6

Spin precession is a common phenomenon in polarized neutron physics. It is of particular importance for the neutron spin-echo technique (NSE) which is substantially different from conventional neutron spectroscopic methods, both conceptually and technically [1,2]. There the energy and momentum transfers taking place due to the scattering process are determined by taking the appropriate difference between the Larmor precession of the neutron spin in a magnetic field in front and behind the sample. Thus the Larmor rotation serves as a kind of internal clock attached to each neutron. In a semi-classical sense this behaviour is described by the well-known Bloch-equation, which relates the pre-

cession angle  $\phi = \gamma BL/v$  of a neutron with velocity  $v$  to the distance  $L$  the neutron traveled within a homogeneous magnetic field  $B$ . There  $\gamma = 2\mu/\hbar = -1.8326 \times 10^8 \text{ s}^{-1}\text{T}^{-1}$  denotes the gyromagnetic ratio of the neutron ( $\mu \dots$  magnetic moment). Due to the Pauli equation, spin and momentum (energy) variables are coupled, which causes the well-known Zeeman shift  $\Delta E = \pm \mu B$  of the kinetic energy of neutrons inside a magnetic field (longitudinal Stern–Gerlach effect). This energy shift has been measured both for transverse and longitudinal field gradients [3,4]. Thus Larmor precession can be considered as the coherent superposition of a spin-up and a spin-down component having slightly different momenta. This means it can be interpreted as an interference phenomenon of the spin-up and the spin-down components of the initial wave packet in the longitudinal direction [5,6]. Therefore, quantum

\* Corresponding author. Tel.: +43 1 588 01 14100; fax: +43 1 588 01 14199; e-mail: rauch@ati.ac.at

optical formulation of neutron interference experiments [7–9] can be adapted easily for the description of spin precession experiments. Since the potential energy of a classical magnetic dipole with perpendicular orientation relative to an applied magnetic field is zero, a purely classical description of spin precession is not appropriate to describe quantum effects like the above mentioned longitudinal Stern–Gerlach effect, albeit almost all other features of spin precession are reproduced correctly. More than this, even a semi-classical approach which describes the neutron spin as a coherent superposition of spin-up and spin-down eigenstates propagating along different trajectories (geometrical optics approach to quantum mechanics, usually referred to as eikonal approximation) is not really sufficient if effects leading to a spatial separation of wave packets become essential. (A thorough discussion of the subtle differences of classical, semi-classical and quantum mechanical description of NSE is found in [10].) However, a spin precession experiment alone, irrespective of whether it is interpreted quantum mechanically or not, is unable to yield the same amount of information like a genuine split-beam interference experiment. Nevertheless there exist situations where it provides complementary insight into physical phenomena which can hardly be gained otherwise. For instance, perfect crystal neutron interferometry could be used to measure the phase shift of the neutron wave function induced by the scalar Aharonov–Bohm (SAB) effect [11]. But since it requires monochromatic neutrons it could not verify the topological character of this effect which implies that the SAB phase shift is nondispersive, i.e. independent of neutron wavelength. A dedicated spin precession experiment [12], on the other hand, allowed an unambiguous demonstration of just this particular feature. It also motivated us to consider in detail the consequences of the implicit interference character of neutron spin precession. An interesting situation arises if, after a certain propagation distance, the spatial separation of the two wave packet components is (much) larger than the coherence length  $\Delta_c = \lambda_0^2/4\pi\delta\lambda$ , where  $\lambda_0$  is the mean wave length and  $\delta\lambda$  is the spectral width of the incident beam. Then in real space there remains no overlap of the two wave packets, which means they are macroscopically distinguishable (e.g. [13]). Evidently Larmor precession then cannot longer

be observed in the usual way because the wave packets do not overlap anymore. A description of this phenomenon in terms of space-time coherence volumes is given in [14]. One might be inclined to call such a delocalized state a Schrödinger-cat-like state [15–17], addressing the problem that an object may exist simultaneously at well separated regions of space. As has been demonstrated in split beam neutron interference experiments [18,19], this loss of spatial interference contrast in real space implies a corresponding interference phenomenon in momentum space. There a characteristic spectrum modulation could be observed when the interference contrast vanished due to spatial phase shifts larger than the coherence length of the neutron beam. The corresponding analogue for spin precession experiments will be reported in this article.

A usual and quite convenient way to visualize the behaviour of such spatially separated states is to use Wigner quasi-distribution functions, which are defined as [20,21]

$$W(x, k) = \frac{1}{2\pi} \int \exp(ik\Delta) \times \psi^* \left( x + \frac{\Delta}{2} \right) \psi \left( x - \frac{\Delta}{2} \right) d\Delta, \quad (1)$$

and which exhibit the feature that integration over one variable gives the distribution function of the other one,

$$\int W(x, k) dk = |\psi(x)|^2 \text{ and} \\ \int W(x, k) dx = |\Phi(k)|^2. \quad (2)$$

The wave function of a beam which propagates in  $\hat{x}$  direction and whose polarization is precessing around the  $\hat{z}$ -axis can be written in the form of a wave packet influenced by the different Zeeman shifts of the parallel and anti-parallel spin components. Under the assumption that the initial polarization is aligned perpendicular to the field, e.g. in the  $+\hat{y}$  direction, for Gaussian momentum distribution centered around

$k_0$  (standard deviation:  $\delta k$ ), one obtains the wave function

$$\psi_{+y} \propto \int \exp \left[ -\frac{(k - k_0)^2}{2(\delta k)^2} \right] (a_{+|+z}\rangle + a_{-|-z}\rangle) dk, \quad (3)$$

where  $a_{\pm} = \exp(i(k_{\pm}x))$  and the Zeeman splitting is described by  $k_{\pm} = k \mp \Delta k$ , with

$$\Delta k = \frac{m\mu B}{\hbar^2 k} \quad \left( \text{and } \Delta k_0 = \frac{m\mu B}{\hbar^2 k_0} \right). \quad (4)$$

Here  $m$  denotes the mass of the neutron. From Eq. (1) it is then straightforward to derive the Wigner

function for such a spin precession in a single homogeneous magnetic field. One ends up with [9]

$$W_{+y}(x, k) \propto [A_+ + A_- + 2A_0 \cos(2x_p \Delta k)] \times \exp \left[ -\frac{(k - k_0)^2}{2(\delta k)^2} \right], \quad (5)$$

where

$$A_{\epsilon} = \exp \left\{ -2(\delta k)^2 \left[ x - x_p \left( 1 + \epsilon \frac{\Delta k_0}{k} \right) \right]^2 \right\}, \quad (6)$$

with  $\epsilon = -1, 0, +1$ . There  $x_p$  denotes the actual distance the neutron has traveled within the field, which is related to the corresponding number of precessions via  $n = x_p \Delta k_0 / \pi$ . Fig. 1 shows the

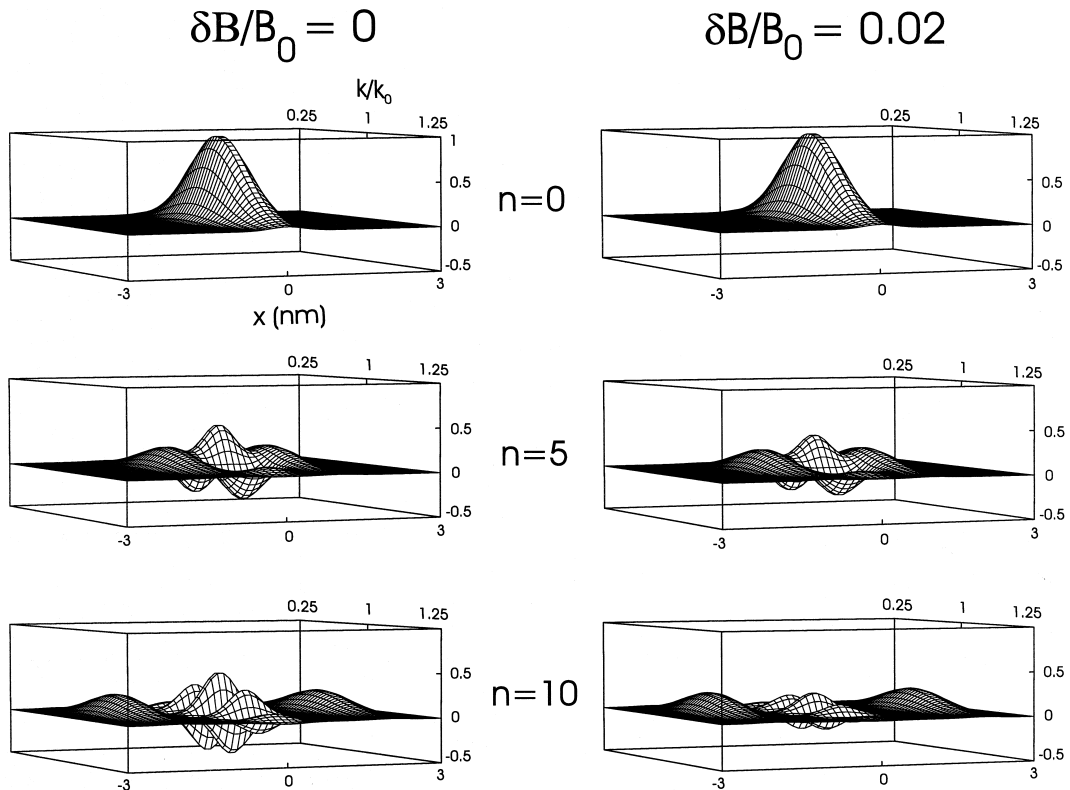


Fig. 1. Calculated Wigner functions of the spin-up part of a polarized neutron beam at the entrance, within and at the exit of the precession field without (left) and with (right) fluctuations ( $\delta B$ ) of the field strength (average value  $B_0$ ) for a fictitiously large Zeeman splitting  $\Delta k_0/k_0 = 10^{-3}$  and a spectral width of the incident beam  $\delta k/k_0 = 10^{-1}$ .  $n$  denotes the number of Larmor precessions. It is related to the travel distance  $x_p$  through the field region and the Zeeman momentum shift  $\Delta k_0$  via  $n = x_p \Delta k_0 / \pi$ .

Wigner function calculated according to Eq. (5) for an (unrealistically) large Zeeman splitting  $\Delta k_0/k_0 = 10^{-3}$  and a spectral width of the incident beam  $\delta k/k_0 = \delta\lambda/\lambda_0 = 10^{-1}$ . According to Eq. (4) such an enormous splitting would require a fictitiously large magnetic field of about 184 T for cold neutrons with a wavelength of about 0.4 nm, which in turn would cause 10 full Larmor precessions at a distance of only 1.85  $\mu\text{m}$ . The appearance of spatially well separated states becomes evident from this figure. Just in between these two states a pronounced wiggle structure in momentum space appears which indicates their non-classical feature. These wiggles are highly fragile against any dissipation and fluctuation effects [8,22,13,23]. This is demonstrated by the right hand side of Fig. 1, where Gaussian fluctuations of the field (or, equivalently, the path length) are taken into account. The disappearance of the wiggles indicates a transition to a mixed state corresponding to a depolarized beam. One encounters the phenomenon described here just at the central position of any type of NSE spectrometer. However, in existing spin-echo systems the Zeeman splitting is much smaller, whereas the spectral width of the beam and the number  $n$  of Larmor precessions are much larger than the values used in Fig. 1. This causes a considerably pronounced fine structure of the wiggles and a still larger spatial separation of the states of typically 150 nm, which is huge compared to their spatial width of about 4 nm. The physical situation within a complete spin echo apparatus,

where a retrieval of the separated states occurs at the exit region of the second precession field, is described in [9].

In the experiment described here the generation of such non-classical quantum states was investigated with a single homogeneous precession field with sufficiently low strength to resolve the wiggles by medium resolution time-of-flight spectroscopy. As mentioned already, the data were taken in the course of an experimental demonstration of the topological nature of the scalar Aharonov–Bohm effect (SAB) at the reactor station Garching [12]. The experimental set-up is sketched schematically in Fig. 2. A chopped polychromatic neutron beam ( $\delta\lambda/\lambda_0 = 0.27$ ) with a mean wavelength  $\lambda_0 = 0.37$  nm non-adiabatically enters and leaves a magnetic field of variable strength ( $B_{\text{max}} \approx 3.5$  mT) which is oriented in  $\hat{z}$ -direction and extends over a length  $L = 0.57 \pm 0.01$  m downstream the beam trajectory ( $\hat{x}$ -axis). This field causes a Zeeman splitting of the wave packet into two components with different momenta, which finally leads to a separation in real space, too. (Here we consider only the case of a static field, since the pulsed field arrangement required for the SAB experiment is of no relevance in the present context.) Initially the beam is polarized along the  $+\hat{y}$  direction by a Co–Ti supermirror; a second supermirror in front of the detector serves to single out the component  $P_y$  of the final polarization vector. A time-of-flight analyzer periodically triggered by the beam chopper records the wavelength distribution of

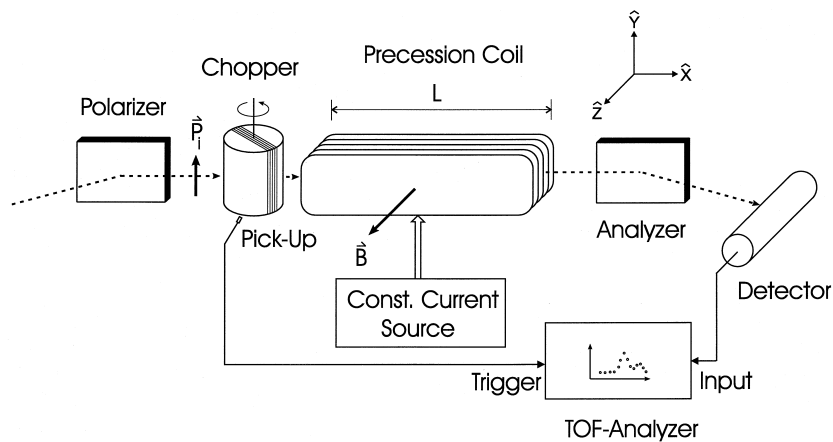


Fig. 2. Schematic sketch of the experimental set up.

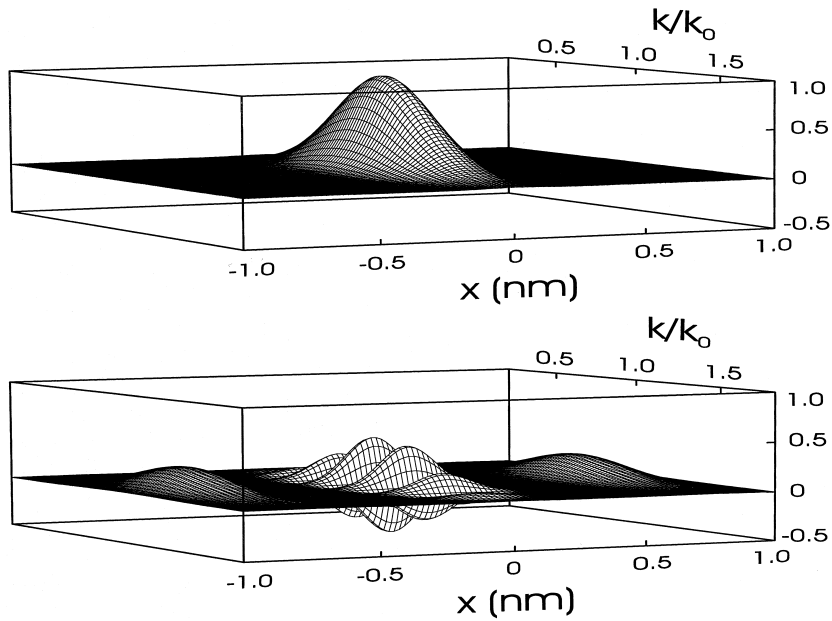


Fig. 3. Theoretically calculated Wigner function at the entrance (*above*) and exit (*below*) of a single magnetic precession field for the chosen parameter set of the experiment.

the transmitted neutrons and thus allows to detect the wiggle structure in momentum (or wavelength) space, which is inevitably associated with the generation of such spatially separated quantum states. In Fig. 3 the Wigner functions at the entrance and the exit position of the precession field are plotted for the chosen experimental parameters ( $B \approx 0.28$  mT). They were calculated from Eq. (5) under the simplifying assumption that the spectral distribution of the incident neutrons is of Gaussian shape. Both the pronounced separation of the states at the exit position and the wiggle structure between them are clearly visible. The spatial separation  $\delta x$  of these two states is about 1.6 nm and exceeds the coherence length  $\Delta_c \approx 0.11$  nm of the incident wave packet by more than an order of magnitude. According to Eq. (2) integration of the Wigner function over the space variable  $x$  yields the momentum distribution of the neutrons which enter and leave the precession field with their polarization aligned along the  $+\hat{y}$  axis. The resulting momentum distribution

$$|\Phi_{+y}(k)|^2 \propto [1 + \cos(2L\Delta k)] \times |\Phi_0(k)|^2 \quad (7)$$

shows a modulation of the incident momentum spectrum  $|\Phi_0(k)|^2$ , where the Zeeman momentum shift

$\Delta k$  is defined by Eq. (4) and  $\Delta k_0/k_0 = 1.4 \times 10^{-6}$ . Experimentally one measures the wavelength distribution of the neutrons via their time-of-flight from

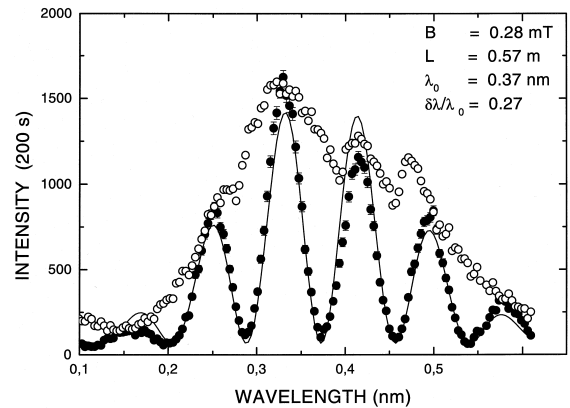


Fig. 4. Comparison of experimentally measured (*full circles*) and theoretically calculated (*full line*) wavelength spectra. The transmission spectrum (*open circles*) measured without any precession field is also shown. (Notice: The deviation from a smooth Maxwell–Boltzmann distribution is just due to the fact that several instruments share the same neutron guide. Insertion of monochromator crystals causes intensity losses at some specific wavelengths.)

the chopper to the detector. Treating the incident wavelength spectrum for reasons of simplicity as Gaussian, one obtains

$$|\Phi_{+y}(\lambda)|^2 \propto \left[ 1 + \cos\left(\frac{\gamma mBL}{h}\lambda\right) \right] \times \exp\left[-\frac{(\lambda - \lambda_0)^2}{2(\delta\lambda)^2}\right]. \quad (8)$$

It can be seen from Fig. 4 that in spite of this simplifying assumption there is a reasonably good agreement between the theoretically calculated and the measured wavelength spectra. In particular the respective positions of the intensity maxima coincide. But it is conclusive that their relative heights cannot be reproduced with similar accuracy. The spectrum measured without precession field is indicated as well in Fig. 4. Notice that the plotted curve is not just a least-squares fit to the experimental data (except, of course, of the background intensity), but is calculated analytically according to Eq. (8) using the specific experimental parameters for  $\lambda_0, \delta\lambda, B$  and  $L$ . At this point a final remark has to be made: the oscillatory behaviour of our wavelength and momentum spectra described by Eqs. (7) and (8) has also been found in atomic beam magnetic resonance [24] and neutron split beam experiments [19] and its origin is similar. But like in the case treated here a purely classical description, though correctly reproducing these oscillations, is only part of the story because the intrinsic coupling of spin and momentum variables requires a more comprehensive treatment. Currently a feasibility study is in progress whether it will be possible to resolve the high frequency wiggle structure of state-of-the art spin-echo spectrometers.

### Acknowledgements

We wish to thank the staff of the reactor station Garching, and in particular Privatdoz. Dr. R. Gähler,

for their invaluable help during the experiments. This project was supported by the TMR European Network (Contract: ERB-FMRX-CT96-0057).

### References

- [1] F. Mezei, *Z. Physik* 2 (1972) 146.
- [2] F. Mezei (Ed.), *Neutron Spin Echo*, Lect. Notes in Physics, Vol. 128, Springer, Berlin, 1980.
- [3] J.E. Sherwood, T.E. Stephenson, S. Bernstein, *Phys. Rev.* 96 (1954) 1546.
- [4] B. Alefeld, G. Badurek, H. Rauch, *Phys. Lett. A* 83 (1981) 32.
- [5] F. Mezei, *Physica B* 151 (1988) 74.
- [6] R. Golub, R. Gähler, T. Keller, *Am.J. Phys.* 62 (1994) 779.
- [7] H. Rauch, *J. Phys. Soc. Jpn.* 65 (1996) 45.
- [8] H. Rauch, M. Suda, *Appl. Phys. B* 60 (1995) 181.
- [9] H. Rauch, M. Suda, *Physica B* 241 (1998) 157.
- [10] R. Gähler, R. Golub, K. Habicht, T. Keller, J. Felber, *Physica B* 229 (1996) 1.
- [11] B. Allman, A. Cimmino, A.G. Klein, G.I. Opat, H. Kaiser, S.A. Werner, *Phys. Rev. Lett.* 68 (1992) 2409.
- [12] G. Badurek, H. Weinfurter, R. Gähler, A. Kollmar, S. Wehinger, A. Zeilinger, *Phys. Rev. Lett.* 71 (1993) 307.
- [13] W. Schleich, M. Pernigo, *Fam Le Kein, Phys. Rev. A* 44 (1991) 2172.
- [14] J. Felber, R. Gähler, R. Golub, K. Prechtel, *Physica B* 252 (1998) 34.
- [15] A. Legett, Proc., *Foundations of Quantum Mechanics in the Light of New Technologies*, S. Kamefuchi (Ed.), Phys. Soc. of Japan, Tokyo, 1984, p. 74.
- [16] B. Yurke, W. Schleich, D.F. Walls, *Phys. Rev. A* 42 (1990) 1703.
- [17] S. Haroche, M. Brune, J.R. Raimond, *Phil. Trans. Roy. Soc. London Ser. A* 355 (1977) 2367.
- [18] H. Rauch, *Phys. Lett. A* 173 (1993) 240.
- [19] D.L. Jacobson, S.A. Werner, H. Rauch, *Phys. Rev. A* 49 (1994) 3196.
- [20] E.P. Wigner, *Phys. Rev.* 40 (1932) 749.
- [21] L. Mandel, E. Wolf, *Optical Coherence and Quantum Optics*, Cambridge Univ. Press, 1995.
- [22] W.H. Zurek, *Phys. Rev. D* 24 (1981) 1516.
- [23] P. Facchi, A. Mariano, S. Pascazio, *Acta Phys. Slovaca* 49 (1999) 677.
- [24] N.F. Ramsey, *Molecular Beams*, Clarendon Press, Oxford, 1956.